Received September 6, 2020, accepted September 21, 2020, date of publication September 25, 2020,
date of current version October 29, 2020.

Digital Object Identifier 10.1109/ACCESS.2020.3026842

Adaptive Fuzzy Control for the Generalized Projective Synchronization of Fractional-Order Extended Hindmarsh-Rose Neurons

DAN LIU[1,2], SONG ZHAO[3], AND XIAOYUAN LUO[1], (Member, IEEE)

[1]Institute of Electrical Engineering, Yanshan University, Qinhuangdao 066004, China
[2]Hebei Key Laboratory of Integrative Medicine on Liver-Kidney Patterns, Institute of Integrative Medicine, College of Integrative Medicine, Hebei University of Chinese Medicine, Shijiazhuang 050200, China
[3]Department of Medical Imaging, The Second Hospital of Hebei Medical University, Shijiazhuang 050000, China

Corresponding author: Xiaoyuan Luo (xyluo@ysu.edu.cn)

This work was supported in part by the National Natural Science Foundation of China under Grant 61873228 and Grant 61903319, and in part by the Science Technology Project of Hebei Province under Grant 20377789D.

ABSTRACT We investigate the generalized projective synchronization (GPS) control of fractional-order extended Hindmarsh-Rose (FOEHR) neuronal models with transcranial magneto-acoustical stimulation (TMAS) input. This improved neuronal model has advantages in describing the complex firing characteristics of neurons stimulated by alternating current. In this study, a master-slave neuron system consisting of two FOEHR neuronal models is assumed to be subject to uncertain model parameters and unknown external disturbances. To quantify the GPS error, we design a new error variable based on the properties of the fractional-order derivative and construct a related GPS error system. Fuzzy logic systems are introduced to approximate the unknown nonlinear dynamics of the error system. To ensure the synchronous firing rhythms of the master-slave neuron system, an adaptive fuzzy control algorithm is proposed under the Lyapunov approach, in which the adaptive parameters are robust to the estimation errors. By choosing the appropriate design parameters, the proposed control scheme enables the master-slave neuron system to achieve GPS in a finite amount of time and to be resilient to uncertain parameters and unknown disturbances. The simulation results demonstrate that after the designed control inputs are implemented, the states of the slave neuron synchronize with those of the master neuron in specified proportions, and the corresponding synchronization error converges towards an arbitrarily small neighborhood of zero.

INDEX TERMS Generalized projective synchronization, fractional-order, extended Hindmarsh-Rose neuronal model, fuzzy logic system.

I. INTRODUCTION

Computational neuroscience plays a crucial role in the understanding of processes in the brain, as it is difficult to identify the actual interactions among neurons in a living brain. The firing characteristics and synchronization behaviors of neurons are closely related to pattern recognition and impulse transmission. Therefore, the modeling and implementation of the synchronization of neurons have received extensive attention from researchers [1].

With the development of computational neuroscience, various neuronal models that represent the biological characteristics of neurons have been proposed, such as the Hodgin-Huxley (HH) [2], FitzHugh-Nagumo (FHN) [3], Hindmarsh-Rose (HR) [4] and Ermentrout [5] neuronal models. The HR neuronal model is commonly used for dynamic analysis and synchronization control of neuronal models. It is a simplified form of the realistic HH model and is expressed by simple polynomials, which facilitates the quantitative calculation of the complex behaviors of neurons. The classical HR neuronal model consists of three variables that represent the membrane potential, the spiking or recovery behavior, and the adaptation current passing through the slow channel, respectively [6], [7]. As research on the biological characteristics of neurons develops, some modified HR neuronal models have been introduced. For example, Lv *et al.* considered the effect of electromagnetic induction and introduced a variable into the HR neuronal model to represent the magnetic flux [8], [9]. Vepa *et al.* proposed an extended HR neuron model consisting of four variables, in which the introduced

The associate editor coordinating the review of this manuscript and approving it for publication was Zhiguang Feng.

variable represents the intracellular interchange of calcium ions between the cytoplasm and its store [10]. The dynamic characteristics of this extended HR neuronal model have been verified to be consistent with the biological characteristics of neurons [11], [12]. Therefore, this improved HR neuronal model is appropriate for the theoretical and computational study of the firing properties and synchronization behaviors of neurons [13], [14].

The classical neuronal models are all expressed by integer-order differential expressions. However, in neuroscience, researchers have found that fractional-order differentiation is more consistent with the firing characteristics of multiple time-scale adaptations for single rat neocortical pyramidal neurons than integer-order adaptations [15]. In addition, the electrophysiological characteristics of brainstem vestibule oculomotor neurons are found to accord better with the fractional-order dynamical properties [16]. In other words, fractional-order neuron models have advantages over integer-order models in terms of their description of neural dynamic behaviors. Therefore, fractional-order neuronal models have been considered in recent research on the firing characteristics and synchronization behaviors of neurons. For example, Yong *et al.* investigated the effect of the fractional order on the firing modes by numerical and simulation analyses and generalized the chaotic characteristics of the fractional-order HR neuronal model [17]. Giresse *et al.* designed a control scheme for the synchronization of FOEHR neuronal models [14]. It is worth noting that these studies consider only direct currents as the external inputs. However, in the treatment of neurological diseases, many noninvasive brain stimulation therapies, such as transcranial magnetic stimulation (TMS) [18], transcranial focused ultrasound stimulation (TFUS) [19] and TMAS [20], generate alternating current as an external input of neurons to change their discharging properties.

In addition to the resting potential, neurons can exhibit periodic spiking, bursting, and chaotic discharge modes with variations in the external forcing current [21]. As the alternating current is determined by the variables of amplitude, frequency and initial phase, the neuronal model with alternating current input has complex dynamic characteristics. TMAS is a relatively new method that utilizes ultrasound waves in a static magnetic field to produce an alternating current as the external stimulation input for neurons [22], [23]. Compared with TMS and TFUS, TMAS has advantages in terms of spatial resolution and penetration depth and has become a potential treatment for neurological diseases [24]. Neurons exposed to TMAS show more complex firing rhythms with different magnetic flux densities, ultrasonic intensities, and fundamental ultrasonic frequencies [24]. Liu *et al.* analyzed the prescribed performance synchronization behaviors of HH neurons under TMAS [25].

According to the biological characteristics of neurons, the types of synchronization for neuron systems include GPS [26], [27], complete synchronization (CS) [25], [28], lag synchronization (LS) [29], anti-phase synchronization (APS) [30], and generalized function projective synchronization (GFPS) [31]. For the nonlinear and chaotic characteristics of neuronal models, various control methods have been applied in the synchronization of neurons, such as feedback control, neural network control, adaptive control, and slide mode control, by using the linear matrix inequality and Lyapunov theory [25], [28], [29], [32]–[34]. For example, Liu *et al.* designed an adaptive neural controller for HH neurons under TMAS to achieve the prescribed performance synchronization [25]. A slide model control scheme with additional conditions was presented for unidirectional complete synchronization of HR neurons in [34]. In [28], some sufficient conditions for the feedback strength and impulsive interval were obtained for the synchronization of two chaotic HR neuron systems. For HR neuron systems subject to asymmetrical time delays, Fan *et al.* discussed how the time delays and coupling strengths affected the lag synchronization and transmission of firing modes between neurons [29]. Vajiheh *et al.* introduced a sliding mode technique for GPS in fractional-order systems and implemented it in classical HR neuronal models [31]. In [13], a feedback synchronization controller was designed for the fractional-order HR neuronal model, whose gain is limited by certain parameter conditions. Later, the authors of [14] designed controllers for the synchronized behavior of coupled fractional-order extended HR neurons. However, these controllers rely on all of the model parameters, this is too strict a requirement for the HR neuronal model, which has uncertain parameters. In addition, unknown external disturbances should also be considered because of their obvious influences on the firing rhythms of neurons.

Based on the above discussion, we explore GPS for FOEHR neuronal models, in which the modeled TMAS alternating current is applied as the external input for computational analysis. To accomplish this goal, an adaptive fuzzy control method is proposed for a master-slave FOEHR neuron system. Under the proposed algorithm, the GPS of the neuron system can be achieved and the neuron system is resilient to model nonlinearity, uncertain parameters, and unknown external disturbances. The contributions of this article are summarized as follows:

1) Compared with previous work [25], [28], [29], [32]–[34], the FOEHR neuronal model considered in this article has advantages in modeling the complex dynamic characteristics of neurons. In addition, an alternating stimulus current is applied in this improved neuronal model, which contributes to the understanding of the mechanism of noninvasive brain stimulation techniques, such as TMAS, which generate alternating currents.

2) A novel fractional-order adaptive controller based on fuzzy logic systems is proposed for the GPS of the two FOEHR neuronal models that are connected in a master-slave configuration. Without loss of generality, these two neuronal models are assumed to have different fractional orders. To the best of our knowledge, GPS control for a master-slave neuron system of heterogeneous

FOEHR neuronal models has not been considered in the literature.

3) The neuron system is assumed to be subject to uncertain model parameters and unknown external disturbances. With the proposed method, the neuronal models can achieve GPS in a finite amount of time and are resilient to uncertain parameters and external disturbances, which are not considered in [14], [32].

The outline of this article is as follows: In Section II, we describe the improved FOEHR neuronal model with TMAS input and introduce fuzzy logic systems to approximate the uncertain sections of the neuron system. In Section III, the GPS problem of the master-slave neuron system of two different FOEHR neuronal models under TMAS is formulated. Then, we propose an adaptive fuzzy control algorithm for the GPS of the neuron system and verify its stability with Lyapunov analysis. The simulations in Section IV guarantee the effectiveness and feasibility of the control scheme. The conclusions are summarized in Section V.

II. MODEL DESCRIPTION AND PRELIMINARIES

A. FRACTIONAL-ORDER DEFINITION AND PROPERTIES

There are various definitions of fractional differentiation, such as the Grunwald-Letnikov definition, the Riemann-Liouville (R-L) definition, and the Caputo definition [35]–[37]. Because the Caputo definition reveals the relationship between the initial condition and the fractional derivative, it will be adopted in this article. The Caputo fractional derivative of a function $x(t)$ is defined as [37]

$$\begin{aligned} {}_0^cD_t^q x(t) &= J_t^{n-q}\left[\frac{d^n}{dt^n}x(t)\right] \\ &= \frac{1}{\Gamma(n-q)}\int_0^t (t-\tau)^{-q+n-1}x^{(n)}(\tau)\,d\tau \end{aligned} \quad (1)$$

where $t \geq 0$, n is the least integer such that $n-1 < q < n$, and $\Gamma(\cdot)$ is the Gamma function.

To simplify the expression, we substitute ${}_0^cD_t^q x(t)$ with $D_t^q x(t)$ for the Caputo operators in the subsequent statements. The following properties of Caputo's fractional derivative will be utilized in the later parts of the paper [37]–[39]:

Property 1: Let $q_1 > 0$, $q_2 > 0$, and $q_1 + q_2 < 1$; then,

$$D_t^{q_1}\left(D_t^{q_2}x(t)\right) = D_t^{q_2}\left(D_t^{q_1}x(t)\right) = D_t^{q_1+q_2}x(t) \quad (2)$$

In particular,

$$D_t^{1-q}\left(D_t^q x(t)\right) = Dx(t) = \frac{d}{dt}x(t) \quad (3)$$

where $0 < q < 1$.

Property 2: The Caputo fractional differential operator satisfies the property of linearity, as follows:

$$D_t^q\left(\mu x(t) + \upsilon y(t)\right) = \mu D_t^q x(t) + \upsilon D_t^q y(t) \quad (4)$$

where μ and υ are real constants. In particular,

$$D_t^q x(t) = D_t^q\left(x(t) + 0\right) = D_t^q x(t) + D_t^q 0 \quad (5)$$

Thus, we have $D_t^q 0 = 0$.

TABLE 1. Value ranges of the magneto-acoustic variables.

Variable of TMAS	Value range
B_x	$[0.5, 5]$(T)
Γ_u	$[0.5, 15]$(W/cm^2)
f_u	$[100, 600]$(kHz)

Property 3: Let $q_1 > 0$, $q_2 > 0$; then,

$$D_t^{q_1}\left(D_t^{-q_2}x(t)\right) = D_t^{q_1-q_2}x(t) \quad (6)$$

In particular,

$$D_t^{q}\left(D_t^{-q}x(t)\right) = x(t) \quad (7)$$

where $q > 0$.

B. MODELED ALTERNATING CURRENT OF TMAS

TMAS is a combination of a static magnetic field and ultrasonic waves acting on neurons. Charged ions in the brain tissue fluid move with the ultrasonic waves when stimulated by TMAS, and are subject to the Lorentz force generated by the magnetic field. The Lorentz force makes charged ions move in the opposite direction, generating an alternating current that has the same frequency as the ultrasonic waves [24]. In addition, the original sinusoidal ultrasound is found to be invalid in generating the sodium current and potential [20]. Therefore, we use a sinusoidal ultrasound wave with an offset as the driving force in this study. The influence of TMAS can be represented by the equivalent current in the neuron system, which can be modeled by

$$I_{ext} = \sigma B_x \sqrt{\frac{2\Gamma_u}{\rho c_0}}\left(\sin(2\pi f_u t) + 1\right) \quad (8)$$

where B_x is the magnetic flux density; σ and ρ are the conductivity and density of brain tissue, respectively; and Γ_u, f_u, and c_0 represent the ultrasonic intensity, ultrasonic frequency, and ultrasonic speed, respectively. In the research on TMAS, the parameters of σ, ρ and c_0 are usually preset to fixed values, and the magneto-acoustic parameters are adjustable variables that should be chosen properly according to the neuromodulation purposes. Based on the theoretical and experimental study of TMAS, the fixed parameters and adjustable ranges of the TMAS parameters are as listed in Table 1 [20]. Since this article focuses on the numerical analysis of the effect of TMAS, the units of the parameters are omitted in the following analysis.

C. THE EXTENDED HINDMARSH-ROSE NEURONAL MODEL WITH THE MODELED TMAS INPUT

The classical HR neuronal model has been widely considered because of its superior computational speed. It has three state variables and can be expressed as follows:

$$\begin{aligned} \dot{x}_1 &= x_2 - ax_1^3 + bx_1^2 - x_3 + I_{ext} \\ \dot{x}_2 &= c - dx_1^2 - x_2 \\ \dot{x}_3 &= r\left(S(x_1 - x_0) - x_3\right) \end{aligned} \quad (9)$$

where x_1 is the membrane potential variable, x_2 is the spiking or recovery variable, and x_3 represents the adaptation current passing through the slow channel. In addition, the small parameter r is introduced to control the rate of change of the slow channel, S is an adjustable parameter, x_0 represents the resting potential, and I_{ext} represents the external stimulus current [4].

With the development of neuronal model research, the classical three-variable HR neuronal model was found to have limits in describing the complex nonlinearity of neurons. For this reason, an improved extended HR neuronal model was proposed in [10], in which a new variable x_4 was introduced to represent the slow intracellular exchange of calcium ions between the cytoplasm and its store. In addition, since the fractional-order differential model has advantages in representing the neuronal dynamic characteristics, as mentioned in the introduction, the extended HR neuronal model with a fractional derivative deserves further research. The FOEHR neuronal model can be represented by [21]

$$\begin{aligned} D_t^q x_1 &= x_2 - a x_1^3 + b x_1^2 - x_3 + I_{ext} \\ D_t^q x_2 &= c - d x_1^2 - x_2 - w x_4 \\ D_t^q x_3 &= r\left(S\left(x_1 - x_0\right) - x_3\right) \\ D_t^q x_4 &= h\left(-p x_4 + f\left(x_2 + g\right)\right) \end{aligned} \tag{10}$$

where the operator D_t^q represents the Caputo fractional derivative. Note that the state variables and model parameters have the same physical meaning as the integer-order HR neuronal model. In this study, the fixed parameters of the FOEHR neuronal model are chosen as follows: $a = 1, b = 3$, $c = 1.01$, $d = 5.0128$, $w = 0.0278$, $r = 0.00215$, $S = 3.966$, $h = 0.0009$, $p = 0.9573$, $f = 3$, $g = 1.619$ and $x_0 = -1.605$.

For the external input I_{ext}, a direct current has been widely considered in the literature [13], [14], [17], [21]. However, in neuroscience, many noninvasive transcranial stimulation methods, such as TMS, TFUS, and TMAS, generate alternating currents to stimulate neurons. In this article, the dynamic characteristics of neurons stimulated by an alternating current are studied by taking the modeled TMAS current as an external input. When the magneto-acoustic parameters are chosen as $B_x = 0.5$, $\Gamma_u = 1.0$, and $f_u = 350.0$ and the fractional order is assumed to be $q = 0.98$, the time evolution of the FOEHR neuronal model with TMAS input is as shown in Figure 1. In this neuronal model, x_1 and x_2 are called fast variables, and the slowly varying parameters can be represented by the variables x_3 and x_4. Similar to the time evolution of variable x_3, when the excitatory cell is inactive and the inhibitory current is absent, the variable x_4 decays slowly to a small value until the neuron system is activated again.

Based on the expression of the TMAS input, both the magnetic flux density and ultrasonic intensity influence the amplitude of the alternating current, and the frequency of the alternating current is consistent with the ultrasonic frequency. Figure 2 shows the interspike intervals (ISIs) of the membrane potentials of the FOEHR neuronal model with different magneto-acoustic parameters. It is obvious that when different magnetic flux densities and ultrasonic intensities are selected, the FOEHR neuronal model exhibits various firing behaviors, such as quiescence, spiking, bursting and chaotic oscillations, but the variable of the ultrasound frequency f_u has little effect on the firing patterns, although it can influence the firing rhythm to a small extent. From these results, we can conclude that the FOEHR neuronal model under alternating stimulus current has more bifurcation parameters and more complex dynamic behaviors than under the direct current that has been studied in the recent literature.

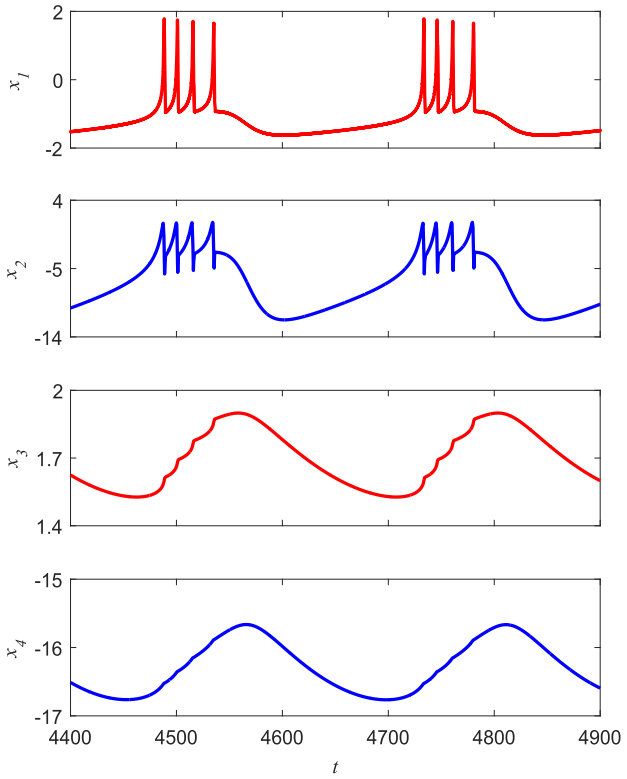

FIGURE 1. Time evolutions of the state variables of the FOEHR neuronal model under TMAS.

D. FUZZY LOGIC SYSTEM APPROXIMATION

To overcome the model uncertainty, fuzzy logic systems were introduced to approximate the unknown parts of the neuron system. A fuzzy logic system consists of a fuzzifier, a fuzzy base, an inference engine, and a defuzzifier [27], [40], [41]. The fuzzifier converts the exact inputs to fuzzy values. The inference engine is considered an important component in the reasoning process, in which the fuzzy values are processed with fuzzy rules. Then, the results are sent to the defuzzifier and converted to crisp values. The fuzzy rules consist of a set of IF-THEN rules that can be expressed as follows:

$$\Re^{(j)}: \text{IF } x_1 \text{ is } A_1^j \text{ and } \ldots \text{and } x_n \text{ is } A_n^j, \text{ THEN } \hat{f}\left(\bar{x}\right) \text{ is } f^j, \tag{11}$$

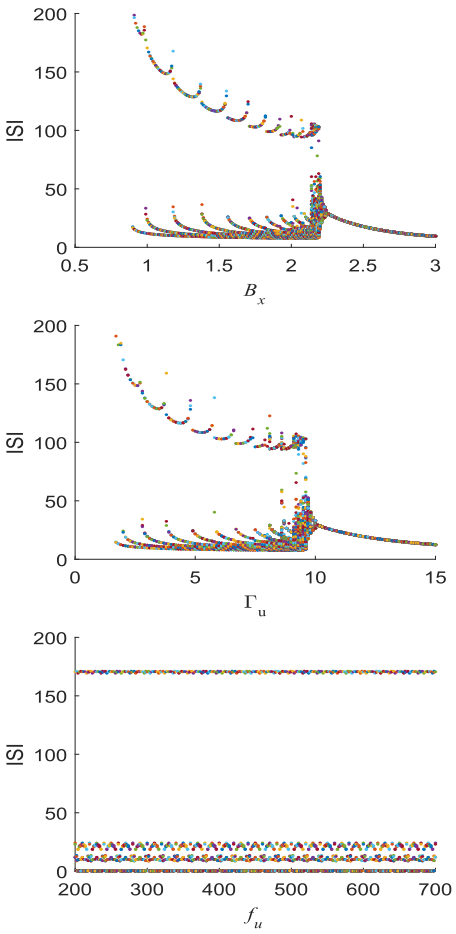

FIGURE 2. ISI diagrams of the membrane potentials of the FOEHR neuronal model with different B_x, Γ_u and f_u.

where $x_1, \ldots, x_n$ are the input variables, $A_1^j, \ldots, A_n^j$ are the fuzzy sets, and f^j is a fuzzy singleton for the output of the jth rule.

A singleton fuzzifier, product inference, and center-average defuzzification method are utilized in this study. The output of the fuzzy logic system can be expressed by

$$\hat{f}(\bar{x}) = \frac{\sum_{j=1}^{l} f^j \left(\prod_{i=1}^{n} \mu_{A_i^j}(x_i)\right)}{\sum_{j=1}^{l} \left(\prod_{i=1}^{n} \mu_{A_i^j}(x_i)\right)} = \theta^T \psi(\bar{x}) \tag{12}$$

where $\bar{x} = [x_1, x_2, \ldots, x_n] \in \Omega_x \subset R^n$, $\mu_{A_i^j}(x_i)$ is the membership function of the variable x_i, $\theta = \left[f^1, f^2, \ldots, f^l\right] \in R^{l \times n}$ and $\psi(\bar{x}) = \left[\psi^1(\bar{x}), \psi^2(\bar{x}), \ldots, \psi^l(\bar{x})\right]^T \in R^{l \times 1}$ are the approximation parameter vector and the fuzzy basis function, respectively. The function $\psi^j(\bar{x}), j = 1, \ldots, l$ can be defined as follows:

$$\psi^j(\bar{x}) = \frac{\left(\prod_{i=1}^{n} \mu_{A_i^j}(x_i)\right)}{\sum_{j=1}^{l} \left(\prod_{i=1}^{n} \mu_{A_i^j}(x_i)\right)} \tag{13}$$

Based on the fuzzy approximation theorem, the optimal approximation parameter vector θ^* is defined on a compact set Ω_θ such that the fuzzy logic system $\theta^{*T}\psi(\bar{x})$ can approximate any nonlinear function $f(\bar{x})$ with arbitrary precision. The minimal approximation error $\varepsilon(\bar{x})$ satisfies

$$f(\bar{x}) = \theta^{*T}\psi(\bar{x}) + \varepsilon(\bar{x}) \tag{14}$$

and $|\varepsilon(\bar{x})| < \bar{\varepsilon}$, where $\bar{\varepsilon}$ is the upper bound of the unknown approximation error. The optimal approximation parameter vector θ^* can be defined by

$$\theta^* = \arg\min_{\theta \subset \Omega_\theta} \left\{ \sup_{\bar{x} \in \Omega_{\bar{x}}} \left| \theta^T \psi(\bar{x}) - f(\bar{x}) \right| \right\} \tag{15}$$

The optimal weight θ^* must be estimated with θ in the control scheme, and the weight estimation error can be defined as $\tilde{\theta} = \theta - \theta^*$.

III. GPS FOR A MASTER-SLAVE NEURAL SYSTEM OF FOEHR NEURONAL MODELS

A. PROBLEM DESCRIPTION

In this study, we consider the GPS problem of two FOEHR neuronal models with TMAS input. The neuron system is constructed in a master-slave configuration, in which the master FOEHR neuronal model is represented by

$$\begin{aligned}
D_t^{q_1} x_{m,1} &= x_{m,2} - a x_{m,1}^3 - b x_{m,1}^2 - x_{m,3} + I_{ext} \\
D_t^{q_1} x_{m,2} &= c - d x_{m,1}^2 - x_{m,2} - w x_{m,4} \\
D_t^{q_1} x_{m,3} &= r\left(S\left(x_{m,1} - x_0\right) - x_{m,3}\right) \\
D_t^{q_1} x_{m,4} &= h\left(-p x_{m,4} + f\left(x_{m,2} + g\right)\right)
\end{aligned} \tag{16}$$

and the slave FOEHR neuronal model, subject to external disturbances and control inputs, is denoted by

$$\begin{aligned}
D_t^{q_2} x_{s,1} &= x_{s,2} - a x_{s,1}^3 - b x_{s,1}^2 - x_{s,3} + I_{ext} + d_1 + u_1 \\
D_t^{q_2} x_{s,2} &= c - d x_{s,1}^2 - x_{s,2} - w x_{s,4} + d_2 + u_2 \\
D_t^{q_2} x_{s,3} &= r\left(S\left(x_{s,1} - x_0\right) - x_{s,3}\right) + d_3 + u_3 \\
D_t^{q_2} x_{s,4} &= h\left(-p x_{s,4} + f\left(x_{s,2} + g\right)\right) + d_4 + u_4
\end{aligned} \tag{17}$$

where $x_{m,i}$ and $x_{s,i}$, $i = 1, 2, 3, 4$, are the state variables of the master and the slave neuronal models, respectively. d_i, $i = 1, 2, 3, 4$, are the unknown external disturbances, which are assumed to have uncertain upper limits $\overline{d}_i$, $|d_i| \le \overline{d}_i$, $i = 1, 2, 3, 4$, and u_i, $i = 1, 2, 3, 4$, represent the designed control inputs. In particular, without loss of generality, we assume that the master and slave neuronal models have different fractional orders, q_1 and q_2. Based on the principle of TMAS, there exists an upper bound of the stimulus current I_{ext}.

B. THE ADAPTIVE FUZZY CONTROL SCHEME

Based on the uncertainty of the neuronal model, the master-slave neuron system can be represented by

$$\begin{aligned}
D_t^{q_1} x_{m,i} &= f_{m,i}(x_m) \\
D_t^{q_2} x_{s,i} &= f_{s,i}(x_s) + d_i + u_i
\end{aligned} \tag{18}$$

where $x_{m,i}$ and $x_{s,i}$, $i = 1, 2, 3, 4$, represent the state variables of the master and slave neuronal model, respectively, and $x_m = \left[x_{m,1}, x_{m,2}, x_{m,3}, x_{m,4}\right]^T \in R^n$ and

$x_s = \left[x_{s,1}, x_{s,2}, x_{s,3}, x_{s,4}\right]^T \in R^n$ are their state vectors. The unknown nonlinear parts of the FOEHR neuronal models are represented by $f_{m,i}$ and $f_{s,i}$, $i = 1, 2, 3, 4$. Our goal is to design GPS control laws u_i that drive the slave variables $x_{s,i}$ to track the time-varying traces of the master state variables in specified proportions, even when they are subject to unknown external disturbances and uncertain model parameters.

To qualify the GPS performance, nonzero scaling factors λ_i, $i = 1, 2, 3, 4$, are introduced and the GPS errors can be defined as $e_i = x_{s,i} - \lambda_i x_{m,i}$.

Remark 1: GPS is a generalized definition of synchronization. When $\lambda_1 = \lambda_2 = \lambda_3 = \lambda_4 = \lambda$, the GPS problem becomes a projective synchronization (PS) problem. In particular, complete synchronization (CS) and anti-phase synchronization (APS) are represented as $\lambda = +1$ and $\lambda = -1$ [42].

To simplify the controller design and stability analysis, new error variables s_i, $i = 1, 2, 3, 4$, are introduced by

$$D_t^{1-q_2} s_i = e_i \tag{19}$$

According to Property 1 and Property 3, the time derivative of the new error variables can be expressed by

$$\dot{s}_i = D_t^{q_2}\left(D_t^{1-q_2} s_i\right) = D_t^{q_2} e_i \tag{20}$$

Substituting (16) into (18), we obtain

$$\dot{s}_i = f_{s,i}(x_s) + d_i + u_i - \lambda_i D_t^{q_2} x_{m,i} \tag{21}$$

The GPS error system can be represented by

$$\dot{s}_i = \varphi_i(x_s, x_m, d_i) + u_i \tag{22}$$

where $\varphi_i(x_s, x_m, d_i) = f_{s,i}(x_s) - \lambda_i D_t^{q_2} x_{m,i} + d_i$, $i = 1, 2, 3, 4$.

Assumption 1: There exists an uncertain continuous positive function vector $\bar{\varphi}_i(x)$ such that

$$|\varphi_i(x_s, x_m, d_i)| \le \bar{\varphi}_i(x) \tag{23}$$

where $x = [x_s, x_m]^T$, $i = 1, 2, 3, 4$.

Remark 2: According to the biological properties of neurons, the state vectors x_s and x_m evolve in a compact set. The unknown external disturbances d_i are assumed to have uncertain upper limits $\bar{d}_i$, and there exists an upper bound of the TMAS current I_{ext}. Thus, Assumption 1 is not restrictive and is consistent with the firing characteristics of neurons.

To overcome the uncertainty of the GPS error system, fuzzy logic systems are introduced to approximate the unavailable nonlinear terms $\bar{\varphi}_i(x)$ with the following equation:

$$\begin{aligned}\bar{\varphi}_i(x) &= \theta_i^{*T}\psi_i(x) + \varepsilon_i(x) \\ &= \theta_i^T\psi_i(x) - \tilde{\theta}_i^T\psi_i(x) + \varepsilon_i(x)\end{aligned} \tag{24}$$

where $\varepsilon_i(x)$, $i = 1, 2, 3, 4$, denote the approximation errors of the fuzzy logic systems and they satisfy $|\varepsilon_i(x)| \le \bar{\varepsilon}_i$, where $\bar{\varepsilon}_i$ represent the unknown upper bounds of the approximation errors.

Next, adaptive parameters k_i, $i = 1, 2, 3, 4$, are introduced to estimate $\bar{\varepsilon}_i$. Then, the estimation errors are $\tilde{k}_i = k_i - k_i^*$, $i = 1, 2, 3, 4$, where k_i^* are the ideal parameters that satisfy $k_i^* = \bar{\varepsilon}_i$.

Assumption 2: There are unknown upper bounds $\bar{\theta}_i$ of the optimal approximation parameters θ_i^* such that $\left\|\theta_i^*\right\| \le \bar{\theta}_i$, $i = 1, 2, 3, 4$.

Remark 3: Assumption 2 is not restrictive, as the upper bounds $\bar{\theta}_i$ are assumed to be unknown and the state vector $x = [x_s, x_m]^T$ of the unavailable nonlinear terms $\bar{\varphi}_i(x)$ is bounded.

According to the biological properties of neurons, the state vectors x_s and x_m evolve in a compact set. The unknown external disturbances d_i are assumed to have uncertain upper limits $\bar{d}_i$, and there exists an upper bound of the TMAS current I_{ext}. Thus, Assumption 1 is not restrictive and is consistent with the firing characteristics of neurons.

For the GPS of the fractional-order master-slave neuron system (16), we design robust adaptive fuzzy control inputs, as follows:

$$u_i = -\theta_i^T\psi_i(x) - k_i - \left(\zeta_i + \left\|\theta_i^T\psi_i(x) + k_i\right\|\right) sat(s_i/h_0) \tag{25}$$

where $\zeta_i > 0, i = 1, 2, 3, 4$ are the design constants, and $sat(s_i/h_0)$ is a piecewise function expressed by

$$sat(s_i/h_0) = \begin{cases} sign(s_i), & |s_i| > h_0 \\ s_i/h_0, & |s_i| \le h_0 \end{cases} \tag{26}$$

where h_0 is a small positive constant that implies a good approximation. Using the control inputs (23) and the fuzzy approximation systems (22), the time derivative of the new error variables can be rewritten as

$$\dot{s} = -\tilde{\theta}_i^T\psi_i(x) - \tilde{k}_i - \left(\zeta_i + \left\|\theta_i^T\psi_i(x) + k_i\right\|\right) sat(s_i/h_0) \tag{27}$$

The adaptive update laws associated with the control inputs can be designed as

$$\dot{\theta}_i = \gamma_{\theta i}\left(s_i\psi_i(x) - \sigma_{\theta i}|s_i|\theta_i\right) \tag{28}$$

$$\dot{k}_i = \gamma_{ki}\left(s_i - \sigma_{ki}|s_i|k_i\right) \tag{29}$$

where $\gamma_{\theta i}$, $\sigma_{\theta i}$, γ_{ki}, and σ_{ki}, $i = 1, 2, 3, 4$, are strictly positive design constants and the initial values of θ_i and k_i satisfy $\theta_i(0) > 0$ and $k_i(0) > 0$, respectively. When the designed control inputs u_i, the adaptive laws $\dot{\theta}_i$ and $\dot{k}_i$ are all applied in the FOEHR neuron system, we can obtain the following main result.

Theorem 1: Consider the master-slave FOEHR neuron system (16) with uncertain model parameters and unknown external disturbances, if Assumption 1 and 2 are satisfied, when the fuzzy control inputs (23) with the adaptive laws (26) and (27) are implemented, all the signals in the closed-loop system are uniformly ultimately bounded, and the synchronization errors e_i can be kept arbitrarily small by selecting the appropriate controller parameters.

Proof: Define the following Lyapunov function candidate:

$$V = \sum_{i=1}^{4} \frac{1}{2} s_i^2 + \sum_{i=1}^{4} \frac{1}{2\gamma_{\theta i}} \left\| \tilde{\theta}_i \right\|^2 + \sum_{i=1}^{4} \frac{1}{2\gamma_{ki}} \tilde{k}_i^2 \quad (30)$$

Differentiating (28) with respect to time, we obtain

$$\dot{V} = \sum_{i=1}^{4} s_i \dot{s}_i + \sum_{i=1}^{4} \frac{1}{\gamma_{\theta i}} \tilde{\theta}_i^T \dot{\theta}_i + \sum_{i=1}^{4} \frac{1}{\gamma_{ki}} \tilde{k}_i \dot{k}_i \quad (31)$$

When $|s_i| > h_0$, substituting (24) and (25) into (29) yields

$$\dot{V} \leq \sum_{i=1}^{4} s_i \left(-\tilde{\theta}_i^T \psi_i(x) - \tilde{k}_i \right) - \sum_{i=1}^{4} \zeta_i |s_i| + \sum_{i=1}^{4} \frac{1}{\gamma_{\theta i}} \tilde{\theta}_i^T \dot{\theta}_i + \sum_{i=1}^{4} \frac{1}{\gamma_{ki}} \tilde{k}_i \dot{k}_i$$

Then, noting the adaptive update laws (26) and (27), we have

$$\dot{V} \leq -\sum_{i=1}^{4} |s_i| \left(\zeta_i + \sigma_{\theta i} \tilde{\theta}_i^T \theta_i + \sigma_{ki} \tilde{k}_i k_i \right) \quad (32)$$

According to Assumption 2 and the definition of adaptive variables k_i, one obtains

$$-\sigma_{\theta i} \tilde{\theta}_i^T \theta_i \leq -\frac{\sigma_{\theta i}}{2} \left\| \tilde{\theta}_i \right\|^2 + \frac{\sigma_{\theta i}}{2} \left\| \theta_i^* \right\|^2 \leq -\frac{\sigma_{\theta i}}{2} \left\| \tilde{\theta}_i \right\|^2 + \frac{\sigma_{\theta i}}{2} \left\| \bar{\theta}_i \right\|^2 \quad (33)$$

$$-\sigma_{ki} \tilde{k}_i k_i \leq -\frac{\sigma_{ki}}{2} \tilde{k}_i^2 + \frac{\sigma_{ki}}{2} k_i^{*2} = -\frac{\sigma_{ki}}{2} \tilde{k}_i^2 + \frac{\sigma_{ki}}{2} \bar{\varepsilon}_i^2 \quad (34)$$

Thus, substituting (31) and (32) into (30) results in

$$\dot{V} \leq -\sum_{i=1}^{4} |s_i| \left(\frac{\sigma_{\theta i}}{2} \left\| \tilde{\theta}_i \right\|^2 + \frac{\sigma_{ki}}{2} \tilde{k}_i^2 + \zeta_i - \frac{\sigma_{\theta i}}{2} \left\| \bar{\theta}_i \right\|^2 - \frac{\sigma_{ki}}{2} \bar{\varepsilon}_i^2 \right) \quad (35)$$

Then if the control parameters ζ_i satisfy the condition that

$$\zeta_i > \frac{\sigma_{\theta i}}{2} \left\| \bar{\theta}_i \right\|^2 + \frac{\sigma_{ki}}{2} \bar{\varepsilon}_i^2 \quad (36)$$

we can conclude that $\dot{V} < 0$, which implies that when $|s_i| > h_0$, $|s_i|$ converges to the set $|s_i| \leq h_0$ within a finite amount of time and thereafter stays in this set. This set is defined as the boundary layer, in which the derivative of the Lyapunov function V can be expressed by

$$\dot{V} \leq -\sum_{i=1}^{4} \frac{\zeta_i}{h_0} s_i^2 - \sum_{i=1}^{4} \sigma_{\theta i} |s_i| \tilde{\theta}_i^T \theta_i - \sum_{i=1}^{4} \sigma_{ki} |s_i| \tilde{k}_i k_i \quad (37)$$

Based on Assumption 2 and the definition of the adaptive variable k_i, we also have

$$-\tilde{\theta}_i^T \theta_i \leq -\left\| \tilde{\theta}_i \right\|^2 + \left\| \tilde{\theta}_i \right\| \left\| \theta_i^* \right\| \quad (38)$$

$$\leq -\left\| \tilde{\theta}_i \right\|^2 + \left\| \tilde{\theta}_i \right\| \bar{\theta}_i \quad (39)$$

$$-\tilde{k}_i k_i \leq -\tilde{k}_i^2 + \tilde{k}_i k_i^* \quad (40)$$

$$\leq -\tilde{k}_i^2 + \tilde{k}_i \bar{\varepsilon}_i \quad (41)$$

Applying these two inequalities to (35), we have

$$\begin{aligned} \dot{V} &\leq -\sum_{i=1}^{4} |s_i| \left[\frac{\zeta_i}{h_0} |s_i| + \sigma_{\theta i} \left(\left\| \tilde{\theta}_i \right\|^2 - \left\| \tilde{\theta}_i \right\| \bar{\theta}_i \right) + \sigma_{ki} \left(\tilde{k}_i^2 - \tilde{k}_i \bar{\varepsilon}_i \right) \right] \\ &= -\sum_{i=1}^{4} |s_i| \left[\sigma_{\theta i} \left(\left\| \tilde{\theta}_i \right\| - \frac{\bar{\theta}_i}{2} \right)^2 + \sigma_{ki} \left(\tilde{k}_i - \frac{\bar{\varepsilon}_i}{2} \right)^2 - \frac{\sigma_{\theta i}}{4} \bar{\theta}_i^2 - \frac{\sigma_{ki}}{4} \bar{\varepsilon}_i^2 + \frac{\zeta_i}{h_0} |s_i| \right] \end{aligned} \quad (42)$$

It is clear that $\dot{V} < 0$ holds as long as

$$|s_i| > \frac{\zeta_i}{h_0} \left(\frac{\sigma_{\theta i}}{4} \bar{\theta}_i^2 + \frac{\sigma_{ki}}{4} \bar{\varepsilon}_i^2 \right) \quad (43)$$

or

$$\left\| \tilde{\theta}_i \right\| > \frac{\bar{\theta}_i}{2} + \sqrt{\left(\frac{\sigma_{\theta i}}{4} \bar{\theta}_i^2 + \frac{\sigma_{ki}}{4} \bar{\varepsilon}_i^2 \right) / \sigma_{\theta i}} \quad (44)$$

or

$$\tilde{k}_i > \frac{\bar{\varepsilon}_i}{2} + \sqrt{\left(\frac{\sigma_{\theta}}{4} \bar{\theta}_i^2 + \frac{\sigma_{ki}}{4} \bar{\varepsilon}_i^2 \right) / \sigma_{ki}} \quad (45)$$

Thus, $\dot{V}$ is negative as long as the controller parameters are defined outside a compact set, which implies that all the signals of the derived error system are bounded. It is demonstrated that the newly defined error variables s_i, fuzzy approximation errors $\tilde{\theta}_i$, and adaptive estimation errors $\tilde{k}_i$, all converge to an adjustable small residual set of zero. Since the residual set depends on the design parameters, the ultimate limit of the signals s_i can be restricted to an arbitrarily small set by choosing appropriate control parameters.

Remark 4: According to the definition of the new error variable s_i and the properties of the fractional-order derivative, there exists positive constants κ_i, $i = 1, 2, 3, 4$, such that $|e_i| \leq \kappa_i |s_i|$, which means that the boundedness of $|e_i|$ can be deduced from the boundedness of $|s_i|$. In particular, $s_i = 0$ implies $e_i = 0$ [42].

From Remark 4 and the demonstration of Theorem 1, we can conclude that the GPS errors e_i can be controlled to converge to an adjustable residual set of zero by applying the proposed control inputs and adaptive laws with the appropriate design parameters, which implies that the firing rhythms of the FOEHR neuronal models achieve GPS.

IV. SIMULATION RESULTS

In this section, some simulations are conducted on the master-slave FOEHR neuron system (16) to verify the availability of the designed control scheme. The fixed parameters of the FOEHR neuronal model are chosen as the parameters in Section II. For the stimulus input I_{ext}, the fixed parameters for tissue fluid and ultrasonic speed are chosen according to Table 1, and the adjustable magneto-acoustic parameters are fixed at $B_x = 0.5$, $\Gamma_u = 1.0$ and $f_u = 350$; then, the exact current can be obtained by equation (9). The initial state vectors of the master and slave neuron system are $x_m(0) = [0.1, 0.2, 0, -0.1]^T$ and $x_s(0) = [0, -0.1, 0.2, -0.6]^T$. The

Adam-Bashforth-Moulton method is applied for the approximate solutions of the fractional-order differentiations and the fractional orders of the master and the slave neuronal models are set to $q_1 = 0.98$ and $q_2 = 0.95$, respectively. The slave neuron is subject to the external dynamic disturbances as follows: $d_1 = 0.8\sin(t)$, $d_2 = 0.5\sin(t)$, $d_3 = 0.05\cos(t)$, and $d_4 = 0.01$.

According to the configuration of the FOEHR neuronal model, four fuzzy logic systems are constructed to approximate the uncertain functions. The membership functions of the fuzzy base are selected as follows: $\mu_{A^j} = \exp\left(-(x-4+j)^2\right)$, $j = 1, 2, \ldots, 7$. The initial values of the adaptive parameters of the fuzzy systems and approximation errors are $\theta_{ij}(0) = 0.1$ and $k_i(0) = 0.1$, respectively. The adaptive vectors θ_i are adjusted by adaptive update laws (26) with $\gamma_{\theta i} = 50$ and $\sigma_{\theta i} = 0.01$, and the adaptive approximation errors k_i are updated by adaptive update laws (27) with $\gamma_{ki} = 10$ and $\sigma_{ki} = 0.01$. Based on the definition of $sat(s_i/h_0)$ and the demonstration of the designed control scheme, the parameter h_0 is related to the coverage speed of the derived GPS error s_i and is chosen as $h_0 = 0.01$. According to Theorem 1, $\zeta_i = 20$ are selected as the proper control parameters to make the control algorithm able to perform GPS for the master-slave neuron system.

In the simulation experiments, CS, APS, and PS are selected as the goals of control. The control inputs are applied to the slave neuron at $t = 1000$ ms, and the time evolutions of the state variables and the synchronization errors of the master and slave neuron system are exhibited to show the synchronization effect. In the state strategies curves, the solid lines represent the time evolution curves of the state variables of the slave neuron, while the dashed lines represent the time evolution curves of the synchronization target, which can be denoted as the product of the state variables of the master neuron $x_{m,i}$ and the synchronization scaling factors λ_i.

(a) Case 1: Complete synchronization (CS)

When $\lambda_1 = 1, \lambda_2 = 1, \lambda_3 = 1$, and $\lambda_4 = 1$, the states of the slave neuron are expected to completely synchronize with the states of the master neuron. Fig. 5 shows the time responses of the state variables of the master and slave neurons. Before the control inputs are implemented, the master and slave neuron have completely different firing rhythms, and the state trajectories of the slave neuron are distorted and irregular, as it is subjected to unknown external disturbances. However, after the controller is applied, the states of the slave neuron immediately track the states of the master neuron. Then, these two coupled neurons have the same state trajectories until the end of the simulation. Fig. 6 shows the time evolutions of the CS errors of the master and slave neuron system. The CS errors of the state variables converge to a small residual set of zero after the control inputs are implemented. Consequently, the proposed adaptive fuzzy controller is robust and can make the master-slave FOEHR neuron system achieve a CS configuration, even in the presence of unknown external disturbances and uncertain dynamics.

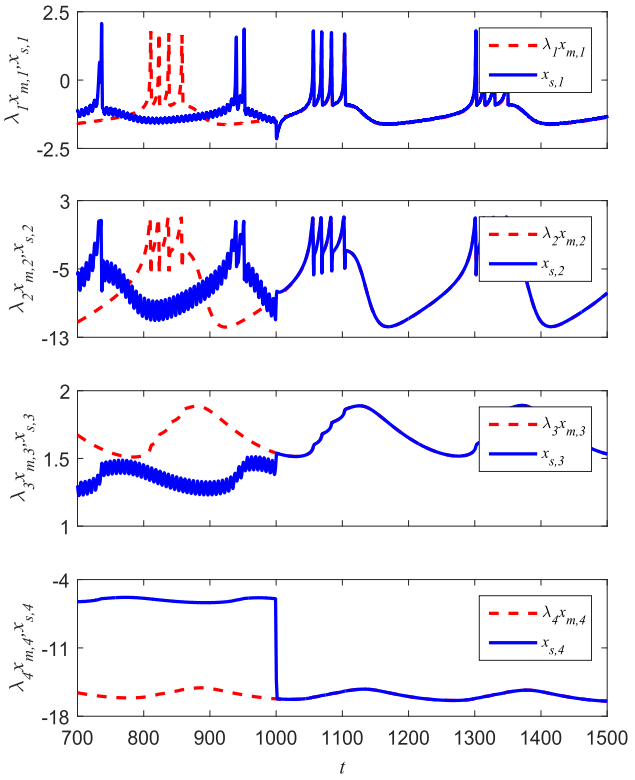

FIGURE 3. Responses of the state variables of the master and slave neuron (CS).

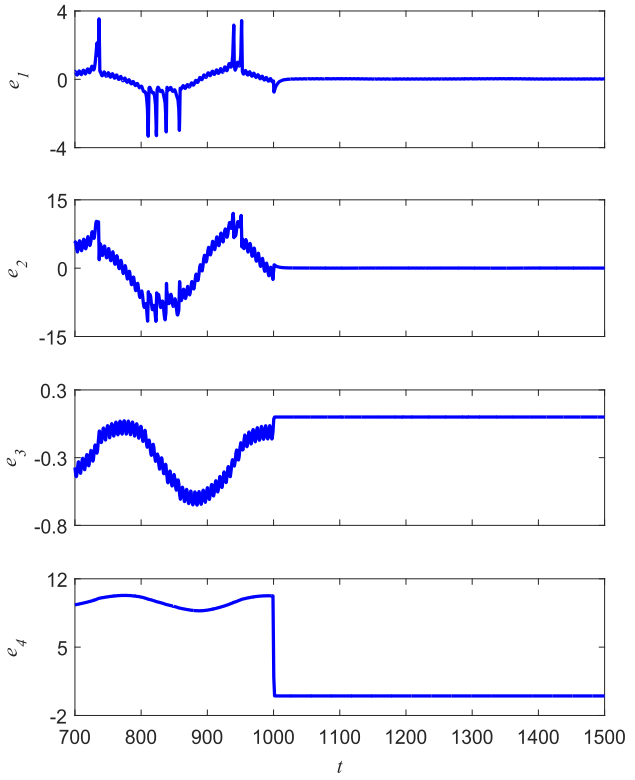

FIGURE 4. Responses of the CS errors of the master-slave neuron system.

(b) Case 2: Anti-phase projective synchronization (APS)

When $\lambda_1 = -0.5, \lambda_2 = -0.5, \lambda_3 = -0.5$, and $\lambda_4 = -0.5$, the master and slave neurons are expected to have anti-phase

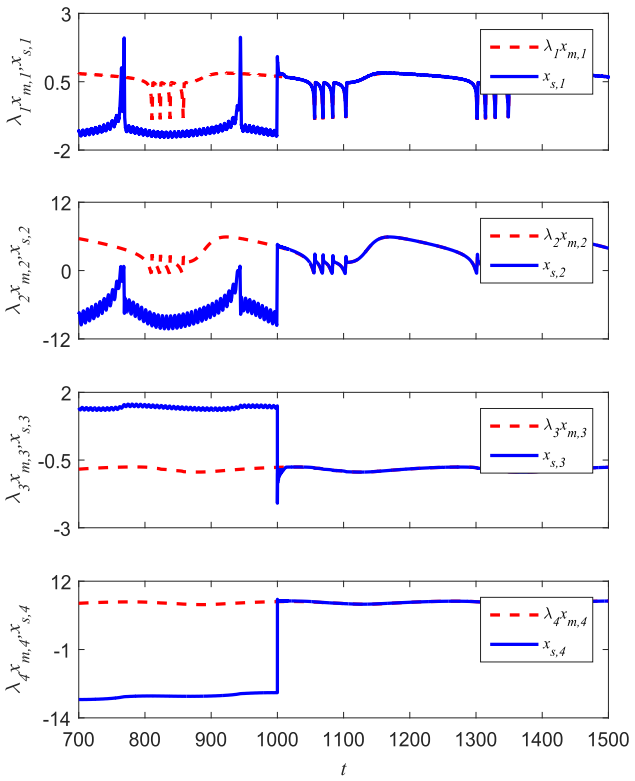

FIGURE 5. Responses of the state variables of the master and slave neuron (APS).

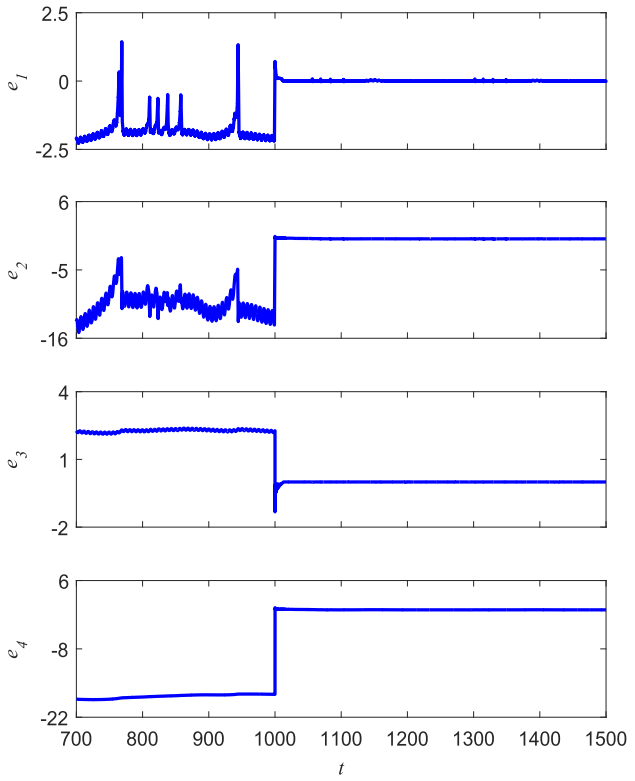

FIGURE 6. Responses of the APS errors of the master-slave neuron system.

state trajectories. The time responses of the states of the master and slave neuron are illustrated in Fig. 7. The slave neuron

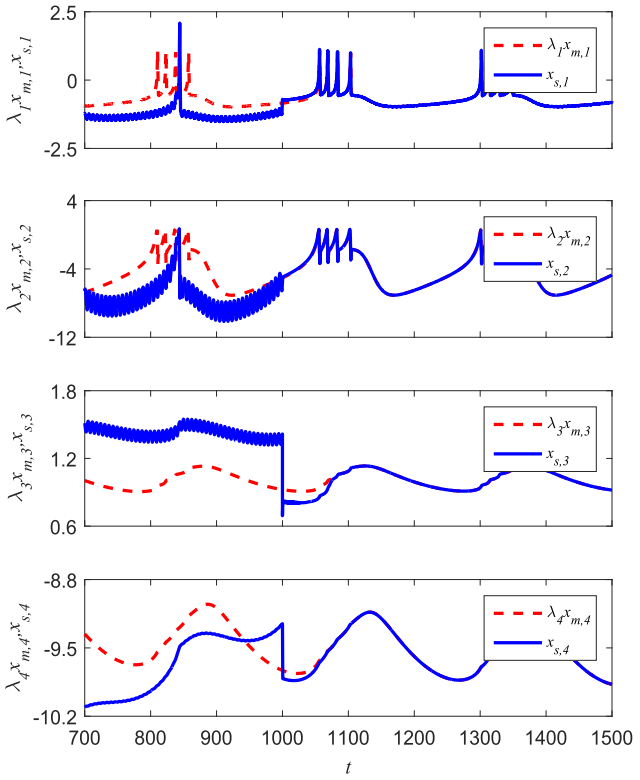

FIGURE 7. Responses of the state variables of the master and slave neuron (GPS).

exhibits distorted and irregular state trajectories without the control inputs. After the control scheme is applied, the slave neuron overcomes the external disturbances immediately and enters a regular state in which the slave neuron has anti-phase states compared with the master neuron, and the amplitudes are reduced in specified proportions. Then, the state trajectories of the master-slave neuron system achieve APS. The time evolutions of the APS errors are depicted in Fig. 8, which shows the desired APS behavior of the two coupled neurons. Thus, the APS of the master-slave neuron system with uncertain dynamics is achieved under the proposed control scheme. Moreover, the adaptive fuzzy control algorithm suppresses the unknown disturbances and causes them to have little influence on the stable synchronization of the coupled neuron system.

(c) Case 3: Projective synchronization (PS)

When $\lambda_1 = 0.6$, $\lambda_2 = 0.6$, $\lambda_3 = 0.6$, and $\lambda_4 = 0.6$, the slave neuron is expected to synchronize with the master neuron in specified proportions. The time responses of the states of the master and slave neuron are depicted in Fig. 9, in which the PS of the neuron system can be observed. When we apply the control scheme, the original irregular state trajectories become ordered states, in which the slave neuron overcomes the external disturbances and its state trajectories track the oscillation trajectories of the state variables of the master neuron proportionally. Then, the master and slave neurons achieve PS. The time evolutions of the PS errors shown in Fig. 10 also verify the PS of these two neurons. It follows that the proposed adaptive fuzzy control scheme is effective

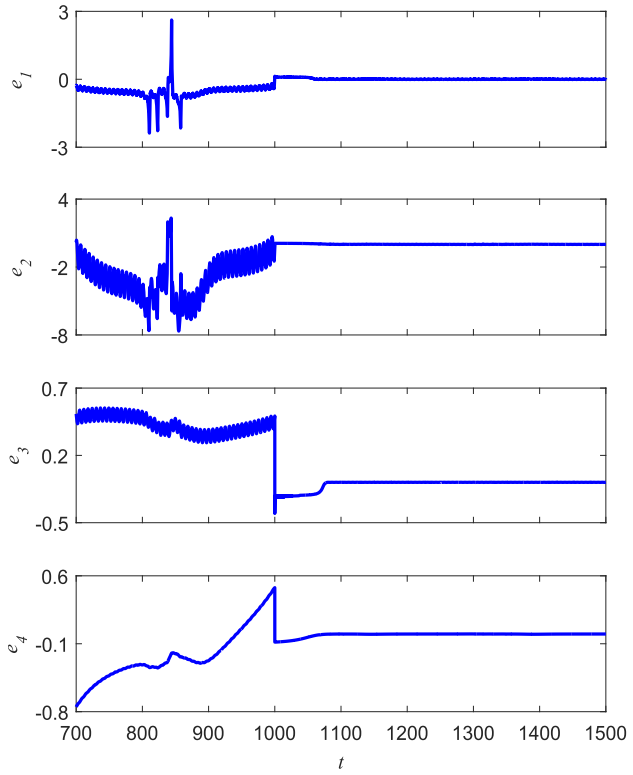

FIGURE 8. Responses of the GPS errors of the master-slave neuron system.

for achieving PS in a master-slave FOEHR neuron system subjected to uncertain dynamics and unknown disturbances.

V. CONCLUSION

In this article, an adaptive fuzzy control algorithm is designed for the GPS problem of a master-slave neuron system that consists of two FOEHR neuronal models with TMAS inputs. The complex firing behaviors and uncertain parameters of the improved neuronal model are considered, and the slave neuron is assumed to be subjected to unknown disturbances. To achieve synchronous behaviors, four new synchronization error variables were introduced to construct a GPS error system. The uncertain nonlinear dynamics of the error system are approximated by fuzzy logic systems, and adaptive variables that are tuned online are utilized to optimize the approximation errors and the approximation weights. When the controller is implemented, the slave neuron is driven to synchronize with the master neuron in specified proportions, and the synchronization errors coverage to zero in a finite amount of time. In the simulation, CS, APS and PS are illustrated to demonstrate the effectiveness of the proposed control method. Our future work will focus on the finite-time lag synchronization problem of fractional-order HR neuronal models.

REFERENCES

[1] I. Belykh, E. de Lange, and M. Hasler, "Synchronization of bursting neurons: What matters in the network topology," *Phys. Rev. Lett.*, vol. 94, no. 18, May 2005, Art. no. 188101.
[2] A. L. Hodgkin and A. F. Huxley, "A quantitative description of membrane current and its application to conduction and excitation in nerve," *J. Physiol.*, vol. 117, no. 4, p. 500, 1952.
[3] R. Fitzhugh, "Impulses and physiological states in models of nerve membrane," *Biophys. J.*, vol. 1, no. 6, p. 455, 1961.
[4] J. L. Hindmarsh and R. M. Rose, "A model of neuronal bursting using three coupled first order differential equations," *Proc. Roy. Soc. London B, Biol. Sci.*, vol. 221, no. 1222, pp. 87–102, Mar. 1984.
[5] B. Ermentrout, "Linearization of F-I curves by adaptation," *Neural Comput.*, vol. 10, no. 7, pp. 1721–1729, Oct. 1998.
[6] M. Storace, D. Linaro, and E. D. Lange, "The Hindmarsh-Rose neuron model: Bifurcation analysis and piecewise-linear approximations," *Chaos*, vol. 18, no. 3, pp. 162–188, 2008.
[7] J. Hizanidis, V. G. Kanas, A. Bezerianos, and T. Bountis, "Chimera states in networks of nonlocally coupled Hindmarsh–Rose neuron models," *Int. J. Bifurcation Chaos*, vol. 24, no. 03, Mar. 2014, Art. no. 1450030.
[8] M. Lv, C. Wang, G. Ren, J. Ma, and X. Song, "Model of electrical activity in a neuron under magnetic flow effect," *Nonlinear Dyn.*, vol. 85, no. 3, pp. 1479–1490, Aug. 2016.
[9] M. Lv and J. Ma, "Multiple modes of electrical activities in a new neuron model under electromagnetic radiation," *Neurocomputing*, vol. 205, pp. 375–381, Sep. 2016.
[10] R. Vepa, "Modelling and estimation of chaotic biological neurons," *IFAC Proc. Volumes*, vol. 42, no. 7, pp. 27–32, 2009.
[11] A. Moujahid, A. d'Anjou, F. J. Torrealdea, and F. Torrealdea, "Efficient synchronization of structurally adaptive coupled Hindmarsh–Rose neurons," *Chaos, Solitons Fractals*, vol. 44, no. 11, pp. 929–933, Nov. 2011.
[12] P. C. Rech, "Dynamics in the parameter space of a neuron model," *Chin. Phys. Lett.*, vol. 29, no. 6, Jun. 2012, Art. no. 060506.
[13] K. Rajagopal, A. J. M. Khalaf, F. Parastesh, I. Moroz, A. Karthikeyan, and S. Jafari, "Dynamical behavior and network analysis of an extended Hindmarsh–Rose neuron model," *Nonlinear Dyn.*, vol. 98, no. 1, pp. 477–487, Oct. 2019.
[14] T. A. Giresse, K. T. Crepin, and T. Martin, "Generalized synchronization of the extended Hindmarsh–Rose neuronal model with fractional order derivative," *Chaos, Solitons Fractals*, vol. 118, pp. 311–319, Jan. 2019.
[15] B. N. Lundstrom, M. H. Higgs, W. J. Spain, and A. L. Fairhall, "Fractional differentiation by neocortical pyramidal neurons," *Nature Neurosci.*, vol. 11, no. 11, pp. 1335–1342, Nov. 2008.
[16] T. J. Anastasio, "The fractional-order dynamics of brainstem vestibulo-oculomotor neurons," *Biol. Cybern.*, vol. 72, no. 1, pp. 69–79, Nov. 1994.
[17] Y. Xie, Y. Kang, Y. Liu, and Y. Wu, "Firing properties and synchronization rate in fractional-order hindmarsh-rose model neurons," *Sci. China Technol. Sci.*, vol. 57, no. 5, pp. 914–922, May 2014.
[18] M. Hallet, "Transcranial magnetic stimulation and the human brain," *Nature*, vol. 406, no. 6792, pp. 147–150, Jul. 2000.
[19] S.-H. Chang, R. Cao, Y.-B. Zhang, P.-G. Wang, S.-J. Wu, Y.-H. Qian, and X.-Q. Jian, "Treatable focal region modulated by double excitation signal superimposition to realize platform temperature distribution during transcranial brain tumor therapy with high-intensity focused ultrasound," *Chin. Phys. B*, vol. 27, no. 7, Jul. 2018, Art. no. 078701.
[20] Y. Yuan, Y. Chen, and X. Li, "Theoretical analysis of transcranial magneto-acoustical stimulation with hodgkin-huxley neuron model," *Frontiers Comput. Neurosci.*, vol. 10, p. 35, Apr. 2016.
[21] D. Jun, Z. Guang-jun, X. Yong, Y. Hong, and W. Jue, "Dynamic behavior analysis of fractional-order Hindmarsh–Rose neuronal model," *Cognit. Neurodyn.*, vol. 8, no. 2, pp. 167–175, Apr. 2014.
[22] Y. Wang, L. Feng, S. Liu, X. Zhou, T. Yin, Z. Liu, and Z. Yang, "Transcranial magneto-acoustic stimulation improves neuroplasticity in hippocampus of Parkinson's disease model mice," *Neurotherapeutics*, vol. 16, no. 4, pp. 1210–1224, Oct. 2019.
[23] S. Liu, X. Zhang, X. Zhou, T. Yin, and Z. Liu, "Experimental study in mice on the technology of transcranial magneto-acoustic coupling electrical stimulation," *J. Biomed. Eng. Res.*, vol. 37, no. 1, pp. 11–15, 2018.
[24] Y. Yuan, Y. Chen, and X. Li, "A new brain stimulation method: Noninvasive transcranial magneto-acoustical stimulation," *Chin. Phys. B*, vol. 25, no. 8, p. 84301, 2016.
[25] D. Liu, S. Zhao, X. Luo, and Y. Yuan, "Unidirectional synchronization of hodgkin-huxley neurons with prescribed performance under transcranial magneto-acoustical simulation," *Frontiers Neurosci.*, vol. 13, p. 1061, Oct. 2019.
[26] S. Vaidyanathan and S. Pakiriswamy, "A 3-D novel conservative chaotic system and its generalized projective synchronization via adaptive control," *J. Eng. ence Technol. Rev.*, vol. 8, no. 2, pp. 52–60, 2015.

[27] A. Boulkroune, A. Bouzeriba, and T. Bouden, "Fuzzy generalized projective synchronization of incommensurate fractional-order chaotic systems," *Neurocomputing*, vol. 173, pp. 606–614, Jan. 2016.
[28] Z. Wang, Y. Jiang, and H. Li, "Impulsive synchronization of time delay bursting neuron systems with unidirectional coupling," *Complexity*, vol. 21, no. 2, pp. 38–46, Nov. 2015.
[29] D. Fan and Q. Wang, "Synchronization and bursting transition of the coupled hindmarsh-rose systems with asymmetrical time-delays," *Sci. China Technol. Sci.*, vol. 60, no. 7, pp. 1019–1031, Jul. 2017.
[30] S. K. Thottil and R. P. Ignatius, "Nonlinear feedback coupling in Hindmarsh–Rose neurons," *Nonlinear Dyn.*, vol. 87, no. 3, pp. 1879–1899, Feb. 2017.
[31] V. Vafaei, H. Kheiri, and A. J. Akbarfam, "Synchronization of fractional–order chaotic systems with disturbances via novel fractional–integer integral sliding mode control and application to neuron models," *Math. Methods Appl. Sci.*, vol. 42, no. 8, pp. 2761–2773, May 2019.
[32] F. Meng, X. Zeng, Z. Wang, and X. Wang, "Adaptive synchronization of fractional-order coupled neurons under electromagnetic radiation," *Int. J. Bifurcation Chaos*, vol. 30, no. 03, Mar. 2020, Art. no. 2050044.
[33] D.-Y. Chen, W.-L. Zhao, X.-Y. Ma, and R.-F. Zhang, "No-chattering sliding mode control chaos in Hindmarsh–Rose neurons with uncertain parameters," *Comput. Math. with Appl.*, vol. 61, no. 10, pp. 3161–3171, May 2011.
[34] Y. Q. Che, J. Wang, K. M. Tsang, and W. L. Chan, "Unidirectional synchronization for hindmarsh-rose neurons via robust adaptive sliding mode control," *Nonlinear Anal. Real World Appl.*, vol. 11, no. 2, pp. 1096–1104, 2010.
[35] I. Petráš, *Fractional-Order Nonlinear Systems: Modeling, Analysis and Simulation*. Cham, Switzerland: Springer, 2011.
[36] B. J. West, "Fractional calculus in bioengineering," *J. Stat. Phys.*, vol. 126, no. 6, pp. 1285–1286, Apr. 2007.
[37] H. Delavari, D. Baleanu, and J. Sadati, "Stability analysis of caputo fractional-order nonlinear systems revisited," *Nonlinear Dyn.*, vol. 67, no. 4, pp. 2433–2439, Mar. 2012.
[38] L. Chen, R. Wu, Y. He, and L. Yin, "Robust stability and stabilization of fractional-order linear systems with polytopic uncertainties," *Appl. Math. Comput.*, vol. 257, pp. 274–284, Apr. 2015.
[39] A. T. Azar, A. Taher, S. Vaidyanathan, and A. Sundarapandian, *Fractional Order Control and Synchronization of Chaotic Systems*. Cham, Switzerland: Springer, 2017.
[40] C. Wu, J. Liu, X. Jing, H. Li, and L. Wu, "Adaptive fuzzy control for nonlinear networked control systems," *IEEE Trans. Syst., Man, Cybern. Syst.*, vol. 47, no. 8, pp. 2420–2430, Aug. 2017.
[41] F. Wang, B. Chen, Y. Sun, Y. Gao, and C. Lin, "Finite-time fuzzy control of stochastic nonlinear systems," *IEEE Trans. Cybern.*, vol. 50, no. 6, pp. 2617–2626, May 2019.
[42] A. Bouzeriba, A. Boulkroune, and T. Bouden, "Fuzzy adaptive synchronization of uncertain fractional-order chaotic systems," *Int. J. Mach. Learn. Cybern.*, vol. 7, no. 5, pp. 893–908, Oct. 2016.

DAN LIU received the master's degree in automation from Yanshan University, China, in 2012, where she is currently pursuing the Ph.D. degree in control theory and control engineering. She is also a Lecturer with the College of Integrative Medicine, Hebei University of Chinese Medicine. Her research interests include dynamic analysis and synchronization control for neuron systems.

SONG ZHAO received the master's degree in imaging and nuclear medicine from Wuhan University, China, in 2013. He is currently a Physician with the Department of Medical Imaging, The Second Hospital of Hebei Medical University. His research interest includes imaging diagnosis of neurological disease.

XIAOYUAN LUO (Member, IEEE) received the Ph.D. degree in control theory and control engineering from Yanshan University, Qinhuangdao, China, in 2005. He is currently a Professor with the Institute of Electrical Engineering, Yanshan University. His current research interests include networked control systems and information processing.